Transactions of the Korean Nuclear Society Spring Meeting
Jeju, Korea, May 18-19, 2017

Corrosion Behavior of SA508 Coupled with and without Magnetite in Chemical Cleaning Environments

Yeong-Ho Son[a,b], Soon-Hyeok Jeon[a], Geun Dong Song[a], Jong-Hyeon Lee[b], Do Haeng Hur[a,*]

[a]*Nuclear Materials Safety Research Division, Korea Atomic Energy Research Institute (KAERI), 989-111 Daedeok-daero, Yuseong-gu, Daejeon 305-353, Republic of Korea*
[b]*Department of Advanced Materials Engineering, Chungnam National University, 99 Daehak-ro, Yuseong-gu, Deajeon, 34134, Republic of Korea*
[*]*Corresponding author: dhhur@kaeri.re.kr*

1. Introduction

Corrosion products released from the surface of the feed water pipe in the secondary water system of pressurized water reactors (PWRs) are mostly magnetite [1]. These corrosion products can lead to various problems, such as the local concentration of chemical impurities within deposits, decrease of heat transfer efficiency, a blockage in waterway, and acceleration of the corrosion of steam generator (SG) materials [2,3].

To mitigate these problems, chemical cleaning process has been widely used. However, the chemical cleaning solution can affect the corrosion of SG structural materials as well as the magnetite dissolution.

Recently, our group has reported that corrosion of nuclear materials is accelerated by a galvanic coupling with magnetite in various secondary water conditions [4-8]. Therefore, during the chemical cleaning process, the galvanic corrosion between SG materials and magnetite is also anticipated because they are in electrical connection. However, the corrosion measurement or monitoring for the materials has been performed without consideration of galvanic effect coupled with magnetite during the chemical cleaning process.

In this study, the effect of temperature and EDTA concentration on the corrosion behavior of SA508 tubesheet material with and without magnetite was studied in chemical cleaning solutions. The galvanic corrosion behavior between SA508 and magnetite is predicted by using the mixed potential theory and its effect on the corrosion rate of SA508 is also discussed.

2. Methods

2.1 Material and Chemicals

SA508 specimens were cut into 10 x 5 x 1 mm for electrochemical tests and 30 x 20 x 1 mm with a 6.5 mm diameter hole for immersion test. SA508 specimens were mechanically ground up to #1000. Chemical composition of SA508 is presented in Table 1.

All corrosion tests were performed in chemical cleaning solutions at 93 °C and immersion test was additionally performed at 121 °C, of which compositions were as follows: 10 and 20 wt.% EDTA, 1 wt.% N_2H_4, 1 wt.% CCI-801 (a corrosion inhibitor). The final pH of all test solutions was adjusted to 7.0 using NH_4OH at 25 °C.

Table 1. Chemical composition of SA508 (wt.%).

C	Si	Mn	P	S	Ni	Cr	Mo	Fe
0.2	0.05	1.52	0.01	0.01	0.99	0.23	0.58	Bal.

2.2 Immersion test

In order to simulate the real galvanic connection between SA508 SG tube sheet and magnetite during the chemical cleaning process, an immersion cell for the galvanic coupling with magnetite powder was newly designed. As shown in Fig. 1, the immersion cell consisted of an upper and lower cap, filtration column, container and coupon hanger made of Teflon and filter was glass fiber. The upper and lower cap of the packed immersion cell was designed to facilitate the filtration of the test solution. Three samples for weight loss measurement and three samples for surface analysis were placed in a coupon hanger. The hanger was located inside the container of the immersion cell. Magnetite powder was packed up to the maximum level of the container because magnetite was rapidly dissolved by the Fe-chelate effect of EDTA. The end part of the thermo-couple and the center of the specimens were set at the same height. In case of SA508 specimen without the magnetite, the coupon hanger and the thermo-couple were also installed in the same method without immersion cell. Each coupled and non-coupled specimen was individually positioned in 750 ml chemical cleaning solution. Weight loss of specimens was measured by using an electronic balance after the immersion test. Corrosion morphology of specimens was also observed by using field emission scanning electron microscope (FE-SEM)

2.3 Electrodeposition of Magnetite

In order to evaluate the electrochemical corrosion behavior of magnetite itself, it is necessary to prepare magnetite specimens. Therefore, thick magnetite film was electrodeposited on the SA508 substrate in $Fe_2(SO_4)_3$ complexed with TEA solution. The resulting gray-green solution was heated to 80 °C. The electrodeposition was conducted at an applied potential of -1.05 V_{SCE} for 10 hours at 80 °C using a PAR273 potentiostat (EG&G). The morphology and chemical composition of magnetite films were analyzed using SEM-energy dispersive X-ray spectroscopy (EDS). The phase identification of magnetite films was analyzed by X-ray diffraction (XRD).

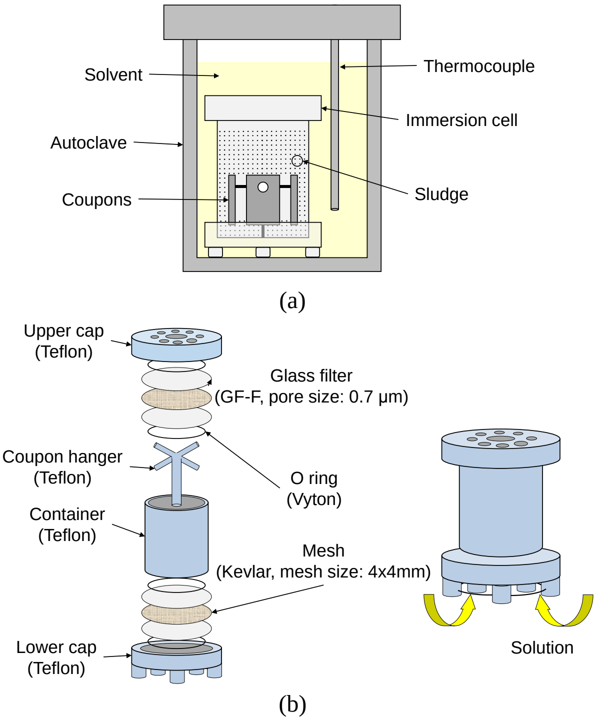

(a)

(b)

Fig. 1. Schematics of details of (a) autoclave and (b) immersion cell in chemical cleaning environments.

2.4 Electrochemical Corrosion test

Two electrochemical techniques were used to study galvanic effect between SA508 and deposited magnetite in 10 % EDTA chemical cleaning solution at 93 °C: potentiodynamic polarization test and zero resistance ammeter (ZRA). A saturated calomel electrode (SCE) and a platinum wire were used as the reference and counter electrode, respectively. The exposed surface area of each SA508 and magnetite specimen was 1.3 cm^2. After the open circuit potential (OCP) was stabilized, polarization scan was started from the OCP to the cathodic or anodic direction with a scan rate of 1 mV/s. The corrosion current density (i_{corr}) of the specimen was calculated by the Tafel-extrapolation of the cathodic and anodic curve between 50 and 100 mV away from the corrosion potential (E_{corr}). The galvanic potential (E_{couple}) and the galvanic current density (i_{couple}) of the galvanic pair were calculated by the mixed potential theory.

The real galvanic corrosion behavior between SA508 and magnetite was also measured by using ZRA for 1800 s. In this case, the area ratio between magnetite and SA508 specimens was equivalent. In addition, the real corrosion current density of non-coupled SA508 was determined by the linear polarization technique (LP) for 1800 s. In this case, the Tafel-slopes of the cathodic and anodic reactions were obtained from the potentiodynamic polarization curves of SA508. The potential was applied from 10 mV more noble to 10 mV more active than the corrosion potential at a scan rate of 0.2 mV/min.

3. Results and Discussion

3.1 Immersion test

Fig. 2 shows the weight loss rate of SA508 obtained by immersion tests. In all conditions, the weight loss rate of coupled SA508 with magnetite powder was 6.6 times higher at 93 °C and 1.7 times higher at 121 °C than that of non-coupled SA508 specimen. The weight loss rate of coupled SA508 specimen also increased with the increase of EDTA concentration at the same temperature. However, although the concentration of EDTA was increased, the weight loss rate of non-coupled specimen was little changed. These results assuredly indicate that the galvanic effect between SA508 and magnetite affected the acceleration of corrosion.

The degree of corrosion rate increase of coupled SA508 specimen at 121 °C was smaller than that at 93 °C. This result may be caused by the insufficient amount of free EDTA acting as Fe-chelate. In previous studies, the effect of EDTA increased as the increase of solution temperature [9-11]. With the increase of solution temperature, more activated EDTA will chelate the Fe-ion from dissolved magnetite. Then, the amount of the free-EDTA affecting the galvanic corrosion is significantly decreased. The reason why the extent of galvanic effect decreases at 121 °C is that immersion tests were performed without the consideration for the reduced amount of free-EDTA in this work.

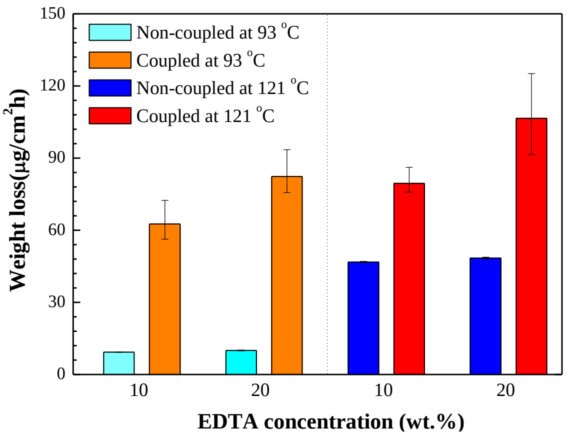

Fig. 2. Effects of magnetite, EDTA concentration, and temperature on the weight loss rate of SA508.

Fig. 3 shows the corrosion morphology of non-coupled and coupled SA508 specimens after the immersion test. As shown in Fig. 3(a) and (b), the specimen in 20 % EDTA at 121 °C was more corroded than that in 10 % EDTA at 93 °C. In coupled SA508 specimen with magnetite, the galvanic effect can be clearly seen in the Fig. 3(c) and (d). Corrosion morphology of SA508 coupled with magnetite was observed severe and non-uniformly corrosion. Coupled SA508 was deeply corroded than non-coupled SA508. Previous researches also showed the similar corrosion morphology in EDTA added test solution [12]. To elucidate the mechanism of this non-uniformly corrosion, more researches will be needed.

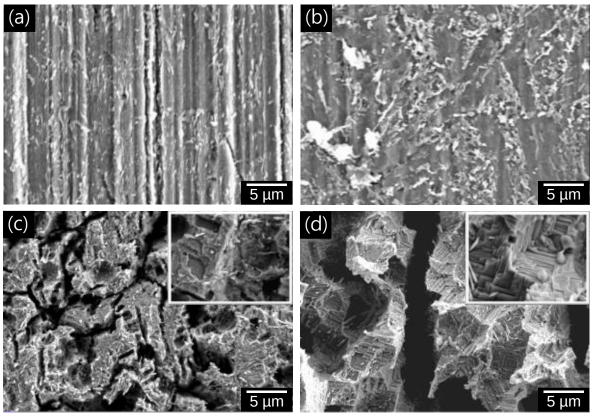

Fig. 3. SEM images showing the corrosion morphology of SA508 after immersion tests: non-coupled SA508 at (a) 93 °C in 10 % EDTA, (b) 121 °C in 20 % EDTA and coupled SA508 with magnetite at (c) 93 °C in 10 % EDTA, (d) 121 °C in 20 % EDTA.

3.2 Electrodeposition of Magnetite

Fig. 4 shows the SEM images of magnetite deposited on the SA508 substrate. The magnetite films had highly faceted and dense morphologies (Fig. 4(a)). This morphology was homogeneous on the whole surface of the deposited magnetite specimen. As shown in Fig. 4(b), the thickness of the magnetite films was about 110 µm. Electrodeposited magnetite was adherent and dense. Crack or hole was not observed at the interface between the magnetite film and SA508 substrate, which confirms that the magnetite film tightly bonded to the SA508 substrate. In addition, the XRD patterns of this layer corresponded to pure crystalline magnetite (JCPDS card no. 19-0629).

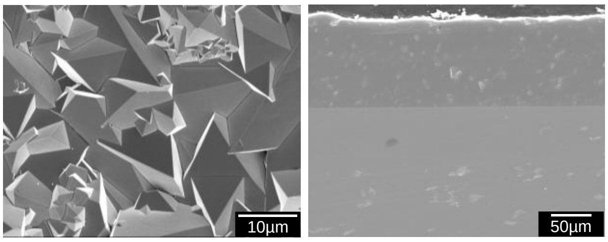

(a) (b)

Fig. 4. SEM images of magnetite film electrodeposited on the SA508 substrate at the applied potential of -1.05 V_{SCE} in the deposition solution at 80 °C for 10 h: (a) top view and (b) cross section.

3.3 Electrochemical Corrosion test

Fig. 5 shows the potentiodynamic polarization curves of SA508 and magnetite specimen in the 10 % EDTA solution at 93 °C. The i_{corr} of SA508 and magnetite at the individual OCPs was calculated from the potentiodynamic polarization curves by means of the Tafel-extrapolation method. The E_{couple} and i_{couple} of the coupling with magnetite were also calculated by means of the mixed potential theory. These electrochemical corrosion parameters are summarized in Table 2. When SA508 and magnetite are electrically contacted, SA508 becomes the anodic element of the galvanic pair because the E_{corr} of SA508 is higher than that of magnetite. As shown in Table 2, the corrosion rate of SA508 will be increased by about 600 times, when they are galvanically contacted to the equivalent area ratio.

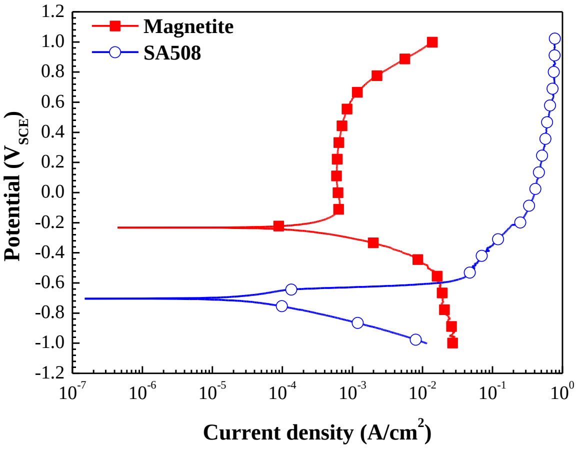

Fig. 5. Polarization curves of SA508 and magnetite in 10 % EDTA solution at 93 °C.

Table 2. Electrochemical corrosion parameters of SA508 and magnetite in 10 % EDTA solution at 93 °C

Corrosion parameters	SA508	Magnetite
E_{corr} (mV_{SCE})	*-704*	*-233*
i_{corr} (mA/cm^2)	*0.028*	*0.171*
E_{couple} (mV_{SCE})	*-599*	
i_{couple} (mA/cm^2)	*16.851*	

Fig. 6 shows the actual E_{couple} and i_{couple} between SA508 and magnetite obtained from ZRA measurement and the real corrosion current density of non-coupled SA508 determined by the LP technique in 10 % EDTA solution at 93 °C. As shown in Fig. 6(a), compared with E_{corr} of non-coupled SA508 at - 700 mV_{SCE}, the actual corrosion potential of SA508 coupled with magnetite was increased to -600 mV_{SCE} due to the galvanic effect. These results show a similar tendency as the predicted result from the mixed potential theory in Table 2. The actual i_{couple} of SA508 specimen was the positive value corresponding to the anodic reaction. This indicates that SA508 specimen is the anode of the galvanic couple, like the result predicted in Fig. 5.

The actual i_{couple} of coupled SA508 has increased by about 600 times than that of non-coupled SA508 as shown in Fig. 6 (b). The above results obtained from ZRA measurement and LP technique show a similar tendency as the result calculated from the mixed potential theory: galvanic coupling between SA508 and magnetite increased the i_{corr} of SA508 by 600 times as shown in Fig. 5 and Table 2.

However, in real nuclear power plants, the ratio of the cathodic to anodic area on the outer surface of SG tube sheet deposited with the porous magnetite is much larger than the equivalent area ratio (1:1) of these electrochemical tests. Therefore, increasing the ratio of cathode to anode area will increase the corrosion rate of anode owing to the area ratio effect.

In this paper, the drastic increase in the corrosion rate of SA508 by the galvanic effect of magnetite was successfully evaluated by the immersion test and predicted by the mixed potential theory and clarified from the ZRA measurement and LP technique. From these results, it is suggested that the galvanic corrosion effect between SA508 and deposited magnetite should be considered when the corrosion monitoring is performed during the chemical cleaning process in steam generators.

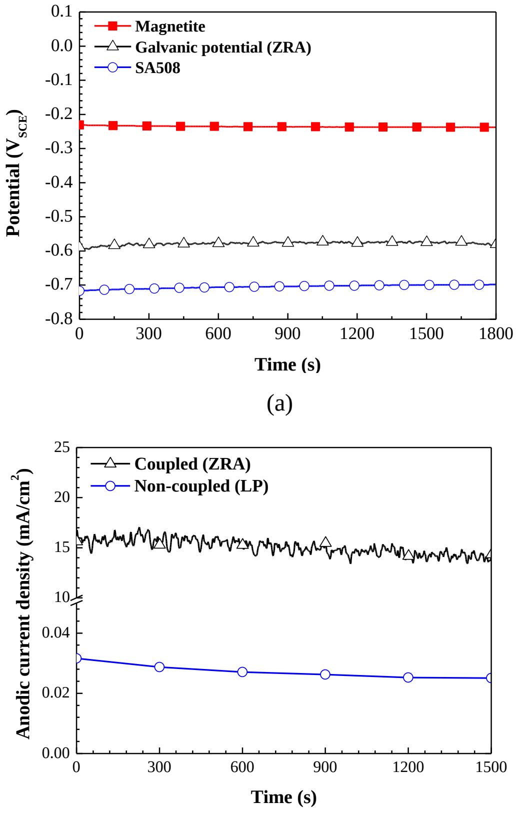

(a)

(b)

Fig. 6. Comparison of (a) corrosion potential and (b) anodic current density of SA508 coupled with and without magnetite in 10 % EDTA solution at 93 °C obtained by ZRA and LP technique.

4. Conclusions

By newly designed immersion test, it was confirmed that the extent of galvanic corrosion effect between SA508 and magnetite increased with increasing temperature and EDTA concentration. The galvanic corrosion behavior of SA508 coupled with magnetite in chemical cleaning environments was predicted by the mixed potential theory and verified by ZRA and LP technique. SA508 was the anode of the galvanic pair because the E_{corr} of the SA508 was lower than that of magnetite. Galvanic coupling increased the corrosion rate of SA508 due to the shift in its potential to the anodic direction. Therefore, the galvanic corrosion effect between SA508 and magnetite should be considered when the corrosion measurement is performed during the chemical cleaning process in steam generators.

ACKNOWLEDGEMENTS

This work was supported by the National Research Foundation of Korea (NRF) grant funded by the Korea government (MSIP) (2017M2A8A4015159).

REFERENCES

[1] R.L. Tapping, C.W. Turner, R.H. Thompson, Corrosion, Vol. 47, p. 489, 1991.
[2] P.M. Scott, Corrosion, Vol. 56, p. 711, 2000.
[3] R.W. Staehle, J.A Gorman, Corrosion, Vol. 59, p. 931, 2003.
[4] S.H. Jeon, G.D. Song, D.H. Hur, Mater. Trans., Vol. 56, p. 2078, 2015.
[5] S.H. Jeon, G.D. Song, D.H. Hur, Metals, Vol. 5, p. 2372, 2015.
[6] G.D. Song, S.H. Jeon, J.G. Kim, D.H. Hur, Corrosion, Vol. 73, p. 216, 2017.
[7] G.D. Song, S.H. Jeon, J.G. Kim, D.H. Hur, Corrosion, Vol. 72, p. 1011, 2016.
[8] S.H. Jeon, G.D. Song, D.H. Hur, Mater. Trans, Vol. 56, p. 1107, 2015.
[9] D.H. Hur, H.S. Chung, U.C. Kim, Nucl. Mater. Vol. 224, p. 179, 1995.
[10] D.H. Hur, M.S. Choi, H.S. Chung, U.C. Kim, Nucl. Mater. Vol. 305, p 220, 2002.
[11] D.H. Hur, M.S. Choi, U.C. Kim, J.H. Han, Nucl. Mater. Vol. 220, p 11, 2003.
[12] A. Kocijan, Mater. Sci. Mater. Med, Vol 14, p 69, 2003.